

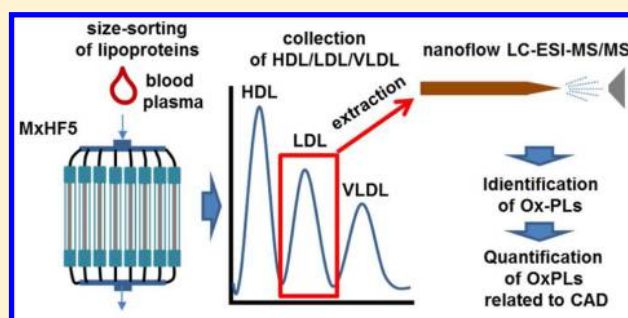
Profiling of Oxidized Phospholipids in Lipoproteins from Patients with Coronary Artery Disease by Hollow Fiber Flow Field-Flow Fractionation and Nanoflow Liquid Chromatography–Tandem Mass Spectrometry

Ju Yong Lee, Seul Kee Byeon, and Myeong Hee Moon*

Department of Chemistry, Yonsei University, Seoul, 120-749, Korea

S Supporting Information

ABSTRACT: Oxidized phospholipids (Ox-PLs) are oxidatively modified PLs that are produced during the oxidation of lipoproteins; oxidation of low density lipoproteins especially is known to be associated with the development of coronary artery disease (CAD). In this study, different lipoprotein classes (high density, low density, and very low density lipoproteins) from pooled plasma of CAD patients and pooled plasma from healthy controls were size-sorted on a semipreparative scale by multiplexed hollow fiber flow field-flow fractionation (MxHF5), and Ox-PLs that were extracted from each lipoprotein fraction were quantified by nanoflow liquid chromatography–tandem mass spectrometry (nLC–ESI-MS/MS). The present study showed that oxidation of lipoproteins occurred throughout all classes of lipoproteins with more Ox-PLs identified from CAD patient lipoproteins: molecular structures of 283 unique PL species (including 123 Ox-PLs) from controls and 315 (including 169 Ox-PLs) from patients were identified by data-dependent collision-induced dissociation experiments. It was shown that oxidation of PLs occurred primarily with hydroxylation of PL; in particular, a saturated acyl chain such as 16:0, 18:0, or even 18:1 at the sn-1 location of the glycerol backbone along with sn-2 acyl chains with at least two double bonds were identified. The acyl chain combinations commonly found for hydroxylated Ox-PLs in the lipoproteins of CAD patients were 16:0/18:2, 16:0/20:4, 18:0/18:2, and 18:0/20:4.



The oxidation of lipoproteins is generally a result of oxidative modification of lipoproteins by lipoxygenase or myeloperoxidase. Recently, medical interest in oxidized low-density lipoproteins (Ox-LDL) revealed that the increased level of Ox-LDL could play a role in the development of coronary artery disease (CAD).^{1,2} Lipoproteins in the blood are globular complexes containing various lipids such as phospholipids (PLs), cholesterol, triacylglycerols (TGs), and others, along with a few proteins. Lipoproteins are classified by their densities as high-density lipoproteins (HDL), LDL, and very low-density lipoproteins (VLDL). Among different lipoproteins, high levels of LDL with size reduction and low levels of HDL are typically known to be indicators of CAD.^{3,4} Since PLs are the major components of lipoproteins, oxidation of lipoproteins primarily results in the formation of oxidized PLs (Ox-PLs), especially in unsaturated fatty acid chains of PLs. Typical products of PL oxidation are long chain products from hydroperoxylation or further to hydroxylation of unsaturated fatty acids and short chain products from the cleavage of unsaturated fatty acyl chains into shorter acyl chains, which are terminated with aldehydes or carboxylic acids or from the formation of lysophospholipids (LPLs). Recent studies show that Ox-PLs may stimulate the aggregation of platelets which is directly involved with atherosclerosis,^{5,6} have a correlation with

pathogenesis of inflammatory disease,⁷ and also induce a change in biological membranes due to the alterations in acyl packing.⁸ Therefore, it is important to elucidate the relationship between the oxidation of PLs and cardiovascular diseases to understand the role of Ox-LDLs.

The structural patterns of Ox-PLs have been investigated with Ox-PC products, which are derived from external oxidation of PC vesicles or LDL particles by electrospray ionization tandem mass spectrometry (ESI-MS/MS) with direct infusion^{9,10} or with liquid chromatography (LC–ESI-MS/MS).^{11–13} While ESI-MS/MS alone offers a high speed analysis of lipids, Ox-PLs are generally low abundance and complicated in structures, requiring separation prior to MS to reduce ion suppression. In our recent report, nanoflow LC–ESI-MSⁿ was utilized for the study of various oxidation patterns of Ox-PLs, including different head groups and isobaric Ox-PL species, which were produced from the external oxidation of PL vesicles and an LDL standard.¹⁴ Use of nLC prior to MS demonstrated that the separation of complicated mixtures of PLs from human plasma and urine samples can be enhanced by

Received: October 24, 2014

Accepted: December 10, 2014

Published: December 10, 2014

setting the limit of detection (LOD) at low fmol/ μL levels, resulting in a decrease of ion suppression from high abundance PL species during ESI.^{15–18} However, for the study of lipoprotein dependent Ox-PLs or Ox-LDLs, HDL and LDL should be isolated prior to the analysis.

In this study, Ox-PL species in different lipoprotein particles of pooled plasma samples from CAD patients and healthy controls were qualitatively and quantitatively profiled. HDL, LDL, and VLDL particles from blood plasma samples were size fractionated and collected at a semipreparative scale by using multiplexed hollow fiber flow field-flow fractionation (MxHF5)¹⁹ in which lipoprotein particles were separated by size. Ox-PLs in each lipoprotein fraction, including intact PLs, were then profiled by nLC–ESI–MSⁿ experiments, and the typical patterns of Ox-PLs found in CAD patients were investigated together with the quantification of Ox-PL species, which showed significant changes between CAD patients and the control group.

EXPERIMENTAL SECTION

Materials and Chemicals. Standard PLs utilized in this study were obtained from Avanti Polar Lipid, Inc. (Alabaster, AL), and their molecular structures were 12:0/12:0-PS (phosphatidylserine), 12:0-LPA (lysophosphatidic acid), 12:0/12:0-PA (phosphatidic acid), 16:0/16:0-PA, 14:0-LPG (lysophosphatidylglycerols), 18:0-LPG, 12:0/12:0-PG (phosphatidylglycerols), 18:0/18:0-PG, 16:0/18:2-PI (phosphatidylinositol), 12:0-LPC (lysophosphatidylcholine), 12:0/12:0-PC (phosphatidylcholine), 14:0/16:0-PC, 14:0-LPE (lysophosphatidylethanolamine), 14:0/14:0-PE (phosphatidylethanolamine), and 18:0/22:6-PE. Lipoprotein standards were obtained from the following: HDL standard from Sigma-Aldrich Co. (St. Louis, MO), LDL standard from Merck Millipore (Darmstadt, Germany), and VLDL standard from Calbiochem (Darmstadt, Germany). HPLC grade solvents (acetonitrile, methanol, isopropanol, and water) were purchased from J. T. Baker (Phillipsburg, NJ). Human plasma samples, including those from 10 healthy Korean individuals and 10 CAD patients (between early 30's and early 50's in ages), were the same as those used in a previous study²⁰ and were obtained from Severance Hospital (Seoul, Korea) under informed consent. Analysis was made with two pooled samples (a pooled control and a pooled patient sample). Fused silica capillaries (20-, 75- μm i.d., 360- μm o.d.) for nLC were purchased from Polymicro Technologies, LLC (Phoenix, AZ).

Multiplexed Hollow Fiber Flow Field-Flow Fractionation (MxHF5). For the assembly of an MxHF5 module, hollow fibers (HF) made up of polyacrylonitrile (PAN) with a molar mass cutoff of 30 kDa from Synopex (Pohang, Korea) were utilized. Each HF (0.85 mm \times 1.55 mm, i.d. \times o.d.) was inserted into a glass tube (2 mm i.d. \times 3 mm o.d. \times 200 mm long) to make an individual HF module, and one end of the glass tube was connected to a Teflon tube by a Teflon tee with $\frac{1}{8}$ in. hand-tight ferrules and nuts from IDEX Health & Science (Oak Harbor, WA). The other end was connected with a Teflon union from IDEX. For the MxHF5, eight HF modules were connected in parallel using a PEEK nine-port manifold from IDEX as shown in Figure 1. The eight outlets of radial flow from each Teflon tee were connected to another PEEK nine-port manifold. For delivery of the carrier solution (0.1 M PBS buffer adjusted to pH 7.4 with 0.27 mM EDTA), a model SP930D solvent delivery pump from Young-Lin Instruments (Anyang, Korea) was used, and a manual loop injector (model

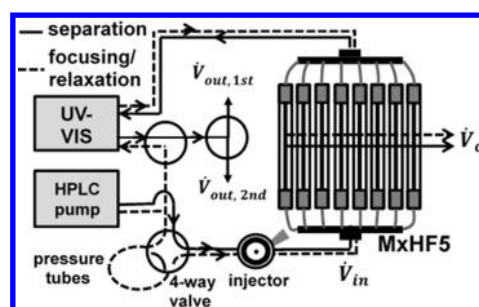


Figure 1. Schematics of the MxHF5 system for semipreparative size sorting of plasma lipoproteins.

7125) from Rheodyne (Cotati, CA) was located before the inlet end of MxHF5 with a sample loop by varying volumes (10, 24, and 80 μL). Monitoring of eluted lipoproteins was performed with a model UV730D UV–vis detector from Young-Lin Instruments at a wavelength of 280 nm for standard lipoproteins and at 600 nm for stained lipoproteins of plasma samples. For the selective detection of lipoprotein particles of plasma samples, the pooled blood plasma sample was stained by mixing with Sudan Black B (SBB) at a ratio of 1:9 (v/v, SBB/plasma) and stirred gently for 1 h at 37 $^{\circ}\text{C}$.

Operation of MxHF5 for the semipreparative scale separation of HDL/LDL/VLDL from plasma samples began by injecting plasma into the injector with the dotted flow paths (injection followed by focusing/relaxation) in Figure 1, and details of the operation are in the Supporting Information.

Lipid Extraction from Lipoprotein Fraction. For the extraction of lipids, including Ox-PLs, from each lipoprotein fraction collected from the MxHF5 run of the pooled plasma sample, the modified Folch method with MTBE/MeOH (methyl-*t*-butylether/methanol)²¹ was employed. Since the polarity of Ox-PLs is relatively increased after oxidation (by addition of oxygen or by acyl chain degradation), a repetitive extraction after adding MTBE consecutively to the mixture was applied when the organic layer was separated from the aqueous layer. Detailed procedures are as follows. The collected lipoprotein fraction contained in an FFF carrier solution was concentrated to 300 μL by an Amicon Ultra-15 centrifugal filter unit from Merck Millipore and then mixed with 300 μL of MTBE and 100 μL of MeOH, followed by vortexing for 10 min. After centrifuging the mixture at 1000g for 5 min for phase separation, the upper organic layer was collected by leaving some of the portion. The lower aqueous layer was mixed with 300 μL of MTBE, followed by the above vortexing, centrifuging, and extracting procedures. This extraction process was repeated twice to maximize the extraction efficiency of Ox-PLs. Collected MTBE solutions were dried under N_2 , and the dried lipid powder was dissolved in $\text{CHCl}_3/\text{MeOH}/\text{water}$ (20:70:10, v/v) and diluted in $\text{CH}_3\text{CN}/\text{water}$ (10:90, v/v) to a final concentration of 5 $\mu\text{g}/\mu\text{L}$.

nLC–ESI–MS/MS. Extracted lipids, including Ox-PLs, from each lipoprotein fraction were analyzed by nLC–ESI–MS/MS, which is composed of a model 1260 Infinity Capillary Pump system equipped with an autosampler from Agilent Technologies (Palo Alto, CA) and a LTQ Velos ion trap mass spectrometer from Thermo Finnigan (San Jose, CA). The analytical column was a homemade capillary column packed with Watchers ODS-P C18 resin (100 \AA , diameter 3 μm) from ISU Industry Co. (Seoul, Korea) in a pulled-tip capillary (75- μm i.d., 360- μm o.d., and 7 cm length). Details of column

preparation similar to a reference¹⁴ are described in the Supporting Information together with the experimental run conditions of nLC–ESI-MS/MS. Identification of PLs and Ox-PLs was performed with LiPilot,²² a computer software developed in our laboratory to identify the molecular structures of PLs from CID spectra. The software is integrated with a library of possible Ox-PL species in which fragment ion patterns were investigated by a study on Ox-PLs produced from oxidation with a Cu^{2+} solution.¹⁴ Validation of searched results was made by manual examination of CID spectra.

RESULTS AND DISCUSSION

Different lipoprotein particles (HDL, LDL, and VLDL) of pooled plasma samples were size-sorted using MxHF5. Flow optimization of MxHF5 to separate all HDL, LDL, and VLDL particles was first performed with a single HF5 module, of which a selected run condition was later expanded to the MxHF5 (8 channels) module. Figure 2 shows separation of

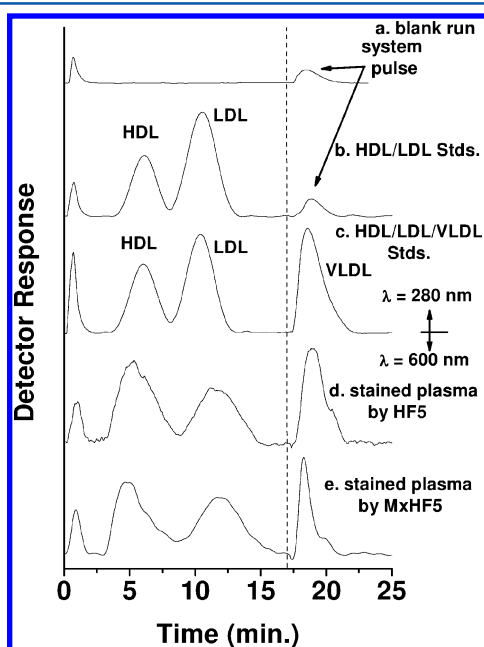


Figure 2. Flow FFF fractograms obtained with the following conditions: (a) blank run using a single HF5 channel during the change in flow rate conditions at 17 min showing a system pulse, (b) separation of a standard mixture of HDL and LDL, (c) separation of HDL, LDL, and VLDL, (d) separation of a human plasma sample stained with SBB, and (e) separation of stained plasma using MxHF5. All runs except run e were obtained with single HF5. Detections of runs a–c were made at 280 nm while runs d and e were at 600 nm.

three lipoprotein particles from single HF5 (a–d) and MxHF5 (e). Since VLDL particles are retained too long at a flow rate condition that was sufficient to separate HDL and LDL, the field strength (or radial flow rate) was decreased with the simultaneous increase of outflow rate from $\dot{V}_{\text{out}}/\dot{V}_{\text{rad}} = 0.24/0.16$ in mL/min to $0.32/0.08$ at 17 min. Figure 2a is the blank run of a single HF5 channel at a step-elution mode showing a system pulse (a small peak) after 17 min when the flow rate was changed. When HDL and LDL standards ($3 \mu\text{g}$ each) were injected to HF5 with the same run conditions, they were well separated with a similar system pulse as shown in Figure 2b. By comparing the area of system pulse peaks in parts a and b of Figure 2, the pulse peak in Figure 2b was expected to originate

from the pressure change during the change of flow rates. Addition of a VLDL standard to the mixture of HDL and LDL standards in Figure 2c yielded successful separation of the three different lipoprotein particles. With these run conditions, $5 \mu\text{L}$ of a human plasma sample stained with SBB was injected into the same HF5 channel showing relatively broad peaks of HDL, LDL, and VLDL in Figure 2d. Staining of the plasma sample was performed to detect lipoproteins selectively at a wavelength of 600 nm without interference by proteins contained in plasma. On the basis of the experiment in Figure 2d, $80 \mu\text{L}$ of the same stained plasma sample was injected for the semipreparative scale separation of lipoproteins in an MxHF5 module at flow rate conditions that were increased 8-fold ($\dot{V}_{\text{out}}/\dot{V}_{\text{rad}} = 3.20/1.92$ in mL/min until 17 min and decreased to $3.20/2.56$). By utilizing the step-elution mode, pooled plasma samples from the CAD patient group and controls were separated without SBB-staining, and each lipoprotein fraction was collected for Ox-PL analysis with nLC–ESI-MS/MS.

Analysis of lipid mixtures that were extracted from each lipoprotein fraction was focused to characterize PLs and Ox-PLs without including neutral lipids such as triacylglycerols (TAGs), diacylglycerols (DAGs), ceramides, and cholesteryl-esters (ChEs). nLC–ESI-MS/MS analysis of the lipid extract samples was performed in both negative and positive ion modes, individually; anionic PLs such as PGs, PIs, PSs, and PAs were performed in negative ion mode, and neutral polar PLs such as PCs and PEs were performed in positive ion mode. Base peak chromatograms of various PL standards (2 pmol each) for different headgroups and chain length can be found in Figure S2 in the Supporting Information obtained in (a) negative ion mode and (b) positive ion mode, in which gradient elution conditions were plotted against the increase in mobile phase B composition. Since oxidation of PLs causes an increase in polarity, Ox-PLs are generally retained shorter than intact PLs. Therefore, ramping of mobile phase B prior to 25 min was done slowly to enhance the separation of complicated Ox-PL mixtures in negative ion mode. However, in positive ion mode, a nearly isocratic condition at 100% B was utilized to separate most PEs and PCs since the peak congestion of Ox-PCs and Ox-PEs of plasma samples was not serious in positive ion mode. Run conditions in Figure S2 in the Supporting Information show that the separation of PLs with different head groups (PA, PG, PI) can be made within 20–40 min while separating regioisomers of 12:0-LPA and 14:0-LPG, which is shown in an inset chromatogram (lyso/12:0-PA for the peak 1a and 12:0/lyso-PA for 1b). Molecular structures of regioisomers can be clearly identified from CID spectra (not shown here) as reported in an earlier report.¹⁶ By using the run conditions in Figure S2 in the Supporting Information, lipid extracts of each lipoprotein fraction from CAD patient plasma and control samples were analyzed, and their BPCs are shown in Figure S3 of the Supporting Information.

Figure 3 shows how Ox-PLs were identified from complicated CID spectra of lipid extracts from the HDL fraction of the pooled CAD patient samples. Figure 3a is an example of an extracted ion chromatogram (EIC), which was plotted with few parent ions based only on specific m/z values and included ions of an intact PI molecule together with three Ox-PI molecules. Figure 3a was extracted from the chromatogram of the HDL fraction shown in Figure S3a of the Supporting Information after identifying a set of Ox-PI species ($18:0/20:4+\text{O}-\text{PI}$ (m/z 901.7), $18:0/20:4+\text{OO}-\text{PI}$ (m/z 917.7), and $18:0/19:5\text{COOH}-\text{PI}$ (m/z 899.6)) along with $18:0/20:4-$

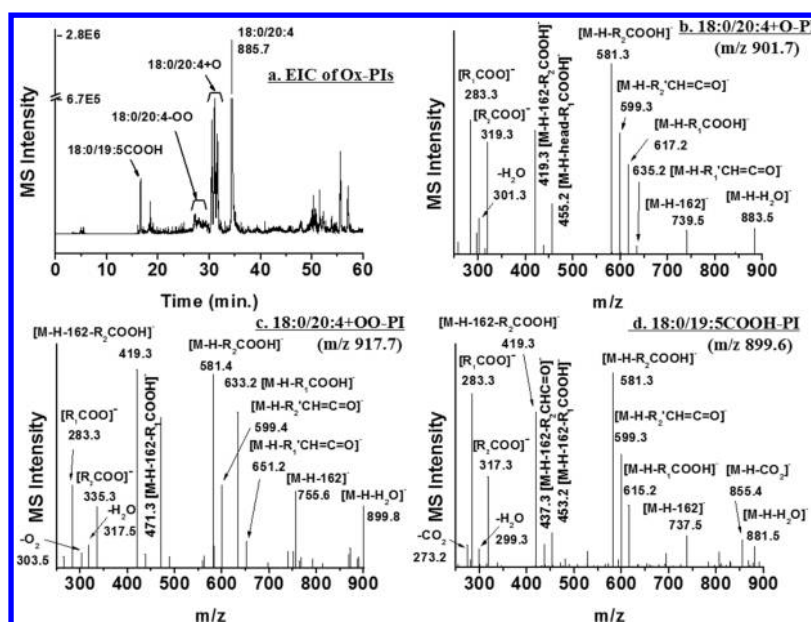


Figure 3. (a) Extracted ion chromatogram based on experimental m/z values identified as an intact 18:0/20:4-PI molecule along with three Ox-PIs from the HDL fraction of the pooled CAD patient plasma samples and CID spectra of the three Ox-PI species: (b) 18:0/20:4+O-PI (m/z 901.7), (c) 18:0/20:4+OO-PI (m/z 917.7), and (d) 18:0/19:5COOH-PI (m/z 899.6) during nLC–ESI-MS/MS experiments.

PI shown as the base peak (m/z 885.7). Compared to the base peak, observed intensities of oxidized products were less than ~25% of the intensity of the base peak; however, most other Ox-PIs found in this study had much lower intensities. Identification of Ox-PI species can be made from the data-dependent CID experiments shown in the following spectra (parts b–d). Figure 3b is the CID spectra of ions with m/z 901.7 eluted at 30–32 min of Figure S3a in the Supporting Information, showing characteristic fragment ions to determine its molecular structure as a singly hydroxylated PI molecule in which one of the bis-allylic position of the sn-2 acyl chain (20:4) is expected to be hydroxylated. Fragment ions of m/z 283.3 ($[R_1COO]^-$) and 319.3 ($[R_2COO]^-$) represent the free carboxylate anions of acyl chains with differentiation of acyl chain location and can be identified from the relative intensity of $[R_1COO]^-$, which is larger than that of $[R_2COO]^-$. The loss of H_2O can be identified from the parent ion as $[M - H - H_2O]^-$ (m/z 883.5) and from free carboxylate ions as $[R_2COO - H_2O]^-$ (m/z 301.3), showing the presence of hydroxide in the sn-2 acyl chain. Loss of the inositol headgroup (162 Da) from the parent ion was shown with ions at m/z 739.5. The characteristic dissociation of acyl chains from the parent ion in the form of ketene or carboxylic acid was found with ions of m/z 635.2 and 599.3 ($[M - H - R_1'CH=C=O]^-$ and $[M - H - R_2'CH=C=O]^-$, respectively) and m/z 617.2 and 581.3 ($[M - H - R_1COOH]^-$ and $[M - H - R_2COOH]^-$, respectively). Moreover, loss of acyl chains from the parent ion without a headgroup ($[M - H - 162 - RCOOH]^-$) was also observed. From these, the molecular structure of the parent ion in Figure 3b was determined as 18:0/20:4+O-PI (+O represents the addition of hydroxide at one of the double bonds in the 20:4 acyl chain); however, the peaks of 18:0/20:4+O-PI in the extracted chromatogram of Figure 3a were shown as triplets due to the presence of positional isomers of 18:0/20:4+O-PI. Since hydroxylation can occur at any bis-allylic position of four double bonds, there can be more than three locations of hydroxylation in the 20:4 acyl chain. The retention time of such positional isomers of single oxidation

was found to decrease as hydroxylation was made at a bis-allylic position farther away from the glycerol backbone according to a previous study.¹⁴

Figure 3c shows CID spectra of another Ox-PI product formed by hydroperoxylation at the sn-2 acyl chain of 18:0/20:4-PI molecules. While the CID spectra show fragment ions having the same m/z values observed in Figure 3b such as $[R_1COO]^-$, $[M - H - R_2COOH]^-$, $[M - H - R_2'CH=C=O]^-$, $[M - H - 162 - R_2COOH]^-$, and $[M - H - 162]^-$, fragment ions produced by the dissociation of sn-1 acyl chains from the parent ion exhibited m/z values 16 Da larger than those found in singly hydroxylated ions: m/z 633.2 for $[M - H - R_1COOH]^-$, m/z 651.2 for $[M - H - R_1'CH=C=O]^-$, and m/z 471.3 for $[M - H - 162 - R_1COOH]^-$. In addition, m/z values of the free carboxylate anions of the sn-2 chain ($[R_2COO]^-$, m/z 335.3) and its dehydrated form ($[R_2COO - H_2O]^-$, m/z 317.5) were increased by 16 Da, supporting the addition of two oxygen (+OO), which can be either from two hydroxylation events or one hydroperoxylation. On the basis of the presence of fragment ions at m/z 303.5 ($[R_2COO - O_2]^-$), this is determined to be hydroperoxylation. Another indication of the presence of peroxide was that possible parent ions having two hydroxides in the sn-2 chain were not detected in the BPC of Figure 3a (due to the difference in polarities, Ox-PIs with two hydroxides will elute earlier than those with one peroxide). However, the split peaks of 18:0/20:4+OO-PI observed at 26–29 min of Figure 3a could originate from the positional isomers of single hydroperoxylation.

Figure 3d represents the CID spectra of a short chain product from a different PI molecule having the same 18:0 at sn-1 but a higher number of carbons and double bonds (possibly 22:6 or 24:6) at sn-2. Though the parent ion in Figure 3d was not produced by oxidation of 18:0/20:4-PI, it was included to show an example of a short chain product. While fragment ions (m/z 581.3 and 599.3), which were produced from the loss of sn-2 acyl chains, were the same as those found in parts b and c of Figure 3, unique fragment ions were detected due to the dissociation of COO from both the

Table 1. Profiling of Oxidized PIs from Each Lipoprotein Class^a

R1/R2 (<i>m/z</i>)	H	L	V	R1/R2 (<i>m/z</i>)	H	L	V	R1/R2 (<i>m/z</i>)	H	L	V
	C/P	C/P	C/P		C/P	C/P	C/P		C/P	C/P	C/P
16:0/16:0(809.7)	/o	o/	o/o	18:2/18:1(859.7)	o/o	o/o	o/o	18:0/18:1CHO(877.3)			/o
16:0/18:0(837.5)	o/o	o/	o/	18:2/18:2(857.6)	o/o	o/o		18:0/18:2+O(877.8)	o/o	o/o	o/o
16:0/18:2(833.6)	o/o	o/o	o/o	18:3/18:2(855.6)		/o		18:0/18:2COOH(891.7)	/o		
16:0/18:3(831.3)	o/o	o/o		20:0/20:4(913.6)			o/	18:0/19:5COOH(899.5)	/o		
16:0/20:3(859.6)		o/		20:5/20:5(901.6)		/o		18:0/20:3+O(903.5)		o/	
16:0/20:4(857.6)	o/o	o/o	o/o	22:2/18:0(917.6)	o/o	o/o	o/	18:0/20:4+O(901.7)	o/o	o/o	o/o
16:0/20:5(855.5)	o/o	/o	o/	22:3/18:0(915.5)	/o			18:0/20:4+2O(917.6)	o/o	o/	o/
16:0/22:6(881.6)	o/o	o/o	o/	22:4/16:0(885.6)			o/	18:0/20:4+OO(917.7)	o/o		
18:0/18:0(865.6)	o/o	o/o	o/o	24:4/18:0(941.5)	/o			18:0/20:5+O(899.6)		/o	
18:0/18:2(861.6)	o/o	o/o	o/o	16:0/lyso(571.1)		o/o	o/o	18:0/21:4CHO(913.7)	o/		
18:0/18:3(859.6)	o/o	/o		16:1/lyso(568.7)			o/	18:0/22:4+O(929.5)	/o	/o	
18:0/20:1(891.7)	/o	/o		lyso/18:0(599)	o/o	/o	/o	18:0/22:5+O(927.5)	o/o		/o
18:0/20:2(889.8)	o/o	o/o	o/	18:0/lyso(599.3)	o/	o/o	o/o	18:1/20:4+O(899.6)	/o		
18:0/20:3(887.7)	o/o	o/o	o/o	lyso/18:1(597.2)	o/o	o/o		17:2CHO/16:0(833.2)			/o
18:0/20:4(885.7)	o/o	o/o	o/o	18:1/lyso(597.2)	/o	/o	o/o	17:2COOH/16:0(849.6)		/o	
18:0/20:5(883.6)	o/o	o/o	o/o	18:2/lyso(595.3)		o/o		18:1COOH+OO/16:0(897.5)	/o		
18:0/20:6(881.6)	o/o	o/o	o/o	lyso/18:3(593.4)		/o	o/	19:4COOH/16:0(873.6)	/o		
18:0/22:4(913.6)	o/o	o/o	o/o	16:0/3:0CHO(641.4)	/o	/o	/o	16:3COOH+O/18:0(877.2)	/o		
18:0/22:5(911.6)	o/o	o/o	o/o	16:0/16:4COOH(831.5)	/o	/o		17:2COOH/18:0(877.4)		/o	
18:0/22:6(909.7)	o/o	o/o	o/o	16:0/17:2COOH(849.8)	/o			17:2COOH+2OO/18:0(941.5)		/o	
18:1/16:0(835.7)	o/o	o/o	o/o	16:0/18:2+O(849.7)		/o	/o	20:4+O and OO/18:0(933.7)		/o	
18:1/16:1(833.5)	o/o	o/o	o/	16:0/20:4+O(873.6)	o/o	o/o	o/o	21:5COOH/18:0(925.5)	/o		
18:1/18:0(863.6)	o/o	o/o	o/o	16:0/22:6+O(897.6)	o/			16:0CHO/18:1(849.6)	o/		
18:1/18:1(861.6)	o/	o/o	o/o	16:0/21:5COOH(899.5)	/o			18:2+O/18:1(875.7)	o/o		
18:1/20:4(883.6)	o/o	o/o	o/	18:0/4:0COOH(699.2)		/o		14:2CHO+OO/18:2(847.5)	/o		
18:1/20:5(881.6)	o/			18:0/6:1COOH(725.3)		/o		16:0CHO/18:2(847.6)	o/o	o/	o/
18:1/22:6(907.5)	o/			18:0/6:2COOH(723.4)		/o		16:0/10:3COOH+OO(781.6)		/o	
18:2/16:0(833.8)		o/	/o	18:0/6:4CHO(701.7)		/o					

^aH, HDL; L, LDL; V, VLDL; C, control; P, patient group.

Table 2. Total Numbers of Identified PLs, Including Ox-PLs^a

species	controls				patients				
	H	L	V	sum	H	L	V	sum	
PI	intact	27	26	25	31	28	27	17	32
	lyso	3	4	5	8	3	7	4	7
	other Ox.	11	6	5	12	21	17	8	34
PA	intact	33	27	24	42	26	19	22	32
	lyso	11	9	7	13	9	11	13	19
	Ox.	11	19	12	23	8	24	15	26
PG	intact	11	13	7	16	13	11	6	15
	lyso	4	3	3	6	4	5	5	7
	other Ox.	2	2	1	3	1	5	5	7
PE	intact	9	9	5	13	9	8	8	13
	lyso	5	7	0	9	9	7	6	10
	other Ox.	1	2	1	3	3	3	2	4
PC	intact	44	41	33	58	32	40	34	54
	lyso	12	17	9	24	16	18	13	21
	other Ox.	10	14	6	22	21	25	14	34
sum	intact	124	116	94	160	108	105	87	146
	lyso	35	40	24	60	41	48	41	64
	other Ox.	35	43	25	63	54	74	44	105

^aH, HDL; L, LDL; V, VLDL.

parent ion and free carboxylic anion such as $[M - H - CO_2]^-$ (*m/z* 855.4) and $[R_2COO - CO_2]^-$ (*m/z* 273.2), respectively. These support the formation of a terminal carboxylic acid at sn-2 chains after truncation of the original acyl chain during oxidation as 18:0/19:5COOH-PI.

Table 1 shows the list of a total of 82 PIs, including oxidized products (Ox-PIs) identified from three different lipoprotein fractions (HDL, LDL, and VLDL) of each pooled control and pooled CAD patient samples: 37 intact PIs, 8 LPIs, and 38 Ox-PIs, which included long chain and short chain products. It was

Table 3. Quantitative Analysis of Oxidized PLs from Each Lipoprotein Class of Pooled Samples^a

m/z	R1	R2	HDL		LDL		VLDL	
			Con.	Pat.	Con.	Pat.	Con.	Pat.
PC								
758.6	16:0	18:2	115.12 ± 24.82	70.82 ± 1.94	52.63 ± 2.09	68.39 ± 2.62	74.03 ± 3.79	46.69 ± 4.07
756.6	16:0	18:3	1.40 ± 0.17	N.D.	2.37 ± 0.11	2.57 ± 0.21	2.61 ± 0.33	N.D.
780.6	16:0	20:5	2.6 ± 0.91	1.98 ± 0.53	0.92 ± 0.22	0.45 ± 0.06	1.02 ± 0.19	13.29 ± 4.33
784.6	18:0	18:3	0.28 ± 0.04	0.14 ± 0.01	0.26 ± 0.03	0.05 ± 0.03	0.35 ± 0.05	0.60 ± 0.07
836.7	22:5	18:0	8.27 ± 0.21	6.35 ± 3.32	N.D.	7.07 ± 1.85	N.D.	0.55 ± 0.11
774.6	16:0	18:2+O	0.61 ± 0.32	8.36 ± 0.53	7.28 ± 0.32	2.55 ± 0.31	N.D.	3.25 ± 0.19
772.6	16:0	18:3+O	0.13 ± 0.02	N.D.	0.02 ± 0.01	0.02 ± 0.0	0.06 ± 0.01	N.D.
796.6	16:0	20:5+O	N.D.	N.D.	0.33 ± 0.17	0.17 ± 0.04	N.D.	2.13 ± 0.12
632.4	16:0	8:2CHO	N.D.	1.30 ± 0.11	N.D.	N.D.	N.D.	N.D.
650.5	16:0	9:0CHO	0.36 ± 0.03	0.96 ± 0.09	N.D.	0.73 ± 0.09	0.50 ± 0.05	N.D.
662.5	16:0	10:1CHO	0.20 ± 0.01	0.31 ± 0.07	N.D.	0.21 ± 0.03	N.D.	0.15 ± 0.02
800.6	18:0	18:3+O	N.Q.	0.06 ± 0.06	N.Q.	N.Q.	N.D.	0.06 ± 0.03
716.5	18:0	12:2CHO	N.D.	0.31 ± 0.04	N.D.	0.42 ± 0.10	0.09 ± 0.01	0.21 ± 0.08
852.7	22:5+O	18:0	1.23 ± 0.21	1.75 ± 0.13	N.D.	0.66 ± 0.30	N.D.	N.D.
PI								
857.6	16:0	20:4	4.04 ± 0.55	3.05 ± 0.29	1.48 ± 0.21	1.98 ± 0.21	2.21 ± 0.15	0.72 ± 0.20
861.6	18:0	18:2	10.62 ± 1.80	5.30 ± 0.87	4.14 ± 1.28	3.03 ± 1.23	5.41 ± 1.77	3.44 ± 1.79
885.7	18:0	20:4	25.57 ± 3.34	16.52 ± 1.30	9.02 ± 0.52	6.75 ± 0.89	19.21 ± 6.50	7.74 ± 0.65
873.6	16:0	20:4+O	0.52 ± 0.08	0.43 ± 0.10	N.Q.	N.Q.	0.10 ± 0.03	0.15 ± 0.05
641.4	16:0	3:0CHO	N.D.	0.29 ± 0.06	N.D.	N.Q.	N.D.	0.17 ± 0.14
897.6	16:0	22:6+O	0.15 ± 0.03	N.D.	N.D.	N.D.	N.D.	N.D.
877.8	18:0	18:2+O	0.52 ± 0.06	0.47 ± 0.03	N.Q.	0.37 ± 0.13	0.05 ± 0.01	0.09 ± 0.02
901.7	18:0	20:4+O	2.07 ± 0.20	3.02 ± 0.52	2.40 ± 0.40	2.49 ± 0.40	2.10 ± 0.55	1.98 ± 0.37
917.7	18:0	20:4+OO	N.Q.	0.63 ± 0.40	N.D.	N.D.	N.D.	N.D.
899.5	18:0	19:5COOH	N.D.	0.23 ± 0.06	N.D.	N.D.	N.D.	N.D.
PG								
745.6	18:2	16:0	2.19 ± 0.89	0.92 ± 0.07	1.55 ± 0.27	1.09 ± 0.33	0.73 ± 0.24	1.39 ± 0.39
761.5	18:2+O	16:0	0.19 ± 0.17	0.40 ± 0.06	N.Q.	0.26 ± 0.28	N.Q.	0.31 ± 0.04
759.7	18:3+O	16:0	N.D.	N.D.	N.Q.	N.Q.	N.D.	0.42 ± 0.09
775.7	18:3+OO	16:0	N.D.	N.D.	N.D.	N.Q.	N.D.	0.18 ± 0.03
PA								
671.5	16:0	18:2	1.95 ± 0.29	1.27 ± 0.09	2.36 ± 0.17	1.78 ± 0.43	0.74 ± 0.18	1.57 ± 0.36
719.5	16:0	22:6	1.32 ± 0.68	0.55 ± 0.26	1.51 ± 0.20	0.09 ± 0.08	0.63 ± 0.25	0.66 ± 0.30
699.5	18:0	18:2	1.52 ± 0.23	1.16 ± 0.45	2.93 ± 0.22	1.72 ± 0.3	0.51 ± 0.29	0.95 ± 0.08
723.6	18:0	20:4	1.88 ± 0.48	0.76 ± 0.24	N.D.	N.D.	N.D.	3.02 ± 0.24
687.5	16:0	18:2+O	0.19 ± 0.05	0.28 ± 0.17	N.Q.	N.Q.	N.Q.	0.18 ± 0.11
709.7	16:0	20:5+O	0.13 ± 0.01	0.13 ± 0.02	N.D.	N.D.	N.D.	0.19 ± 0.05
737.5	16:0	22:5+O	N.D.	N.D.	0.03 ± 0.03	0.17 ± 0.09	N.D.	N.D.
735.6	16:0	22:6+O	N.Q.	N.D.	N.Q.	N.Q.	0.05 ± 0.05	0.06 ± 0.04
715.5	18:0	18:2+O	0.26 ± 0.10	0.24 ± 0.12	0.33 ± 0.11	0.53 ± 0.26	N.D.	0.24 ± 0.15
739.6	18:0	20:4+O	N.Q.	N.Q.	N.Q.	N.Q.	N.D.	0.78 ± 0.12
763.6	18:0	22:6+O	N.Q.	N.D.	N.D.	0.11 ± 0.09	N.D.	0.21 ± 0.05

^aOx-PLs for quantification were selected from the list in Table S1 in the Supporting Information showing significant changes between control and patient samples. The written values are the relative peak area ratio ($n = 3$) compared to that of an internal standard. 12:0/12:0-PC and 12:0/12:0-PS were used as internal standards for positive ion mode and negative ion mode, respectively. N.D., not detected; N.Q., not quantified.

shown from experiments that acyl chains of 16:0, 18:0, and 18:1 were found mostly in the sn-1 location, and oxidations primarily occurred in acyl chains having two or more double bonds. In addition, most oxidations occurred with PI molecules having a saturated acyl chain (16:0 or 18:0), except in a few cases (18:2+O/18:1, 18:1/20:4+O, etc.). While intact PIs were found throughout all lipoprotein classes of both control and patient samples, lyso-PIs (or LPIs) were found randomly, and most Ox-PIs were identified exclusively from a specific lipoprotein class of patient samples except 18:0/18:2+O, 18:0/20:4+O, and 16:0/20:4+O, which were identified in both groups. It is clearly shown that the majority of oxidized PI

products found in this study originated from the CAD patient sample, supporting that hydroxylation occurred widely on lipoproteins in CAD patients. The total numbers of Ox-PIs identified were 12 and 34 from control and patient samples, respectively. Identification of other PL classes was also performed, and the results are listed in Table S1 of the Supporting Information. The numbers of identified PLs and Ox-PLs in each lipoprotein fraction from the control and patient samples are summarized in Table 2, which was classified by intact PL, LPL, and other Ox-PL. In total, 283 unique PL species (160 intact PLs, 60 LPLs, and 63 other Ox-PLs) were identified from the control sample while 315 unique PLs (146

intact PLs, 64 LPLs, and 105 other Ox-PLs) were identified from the patient sample. Comparison of the number of Ox-PL species supports that oxidation of PLs is strongly related to CAD. In addition, oxidation of PLs not only occurred in LDL but also throughout all classes of lipoproteins.

The quantification of Ox-PL species along with their corresponding intact PL molecules was performed by calculating the peak area of each precursor ion. Table 3 lists the quantified Ox-PLs contained in each lipoprotein class together with their corresponding intact PL molecules that are supposed to be the precursors. Since the concentrations of most Ox-PL species were relatively low compared to those of intact PLs, few Ox-PL species were selected for quantification together with their expected original PL species (marked in bold) in Table 3. Since MS intensity of PL molecule depends on the type of head groups and the length of acyl chain together with the degree of unsaturation, a relative quantitation of PLs as well as Ox-PLs was carried out. Therefore, measured data reported in Table 3 were based on relative peak intensity with respect to each internal standard (100 fmol each for 12:0/12:0-PC and 12:0/12:0-PS at positive and negative modes, respectively) to the extracted samples for relative quantitation of the PLs and Ox-PLs. In particular, 16:0/18:2+O-PC was observed with a significant increase (~15-fold) in HDL from the patient group, with an almost 3-fold decrease in LDL. Moreover, it appeared in VLDL from the patient group, though it was not found in VLDL from the control group. The amount of original PC molecules (16:0/18:2-PC) from which 16:0/18:2+O-PC was presumed to be oxidized was much higher in all lipoprotein classes than those of other PC species, and it was found to decrease in HDL (70.82 ± 1.94 from 115.12 ± 24.82 of control) and VLDL (46.69 ± 4.07 from 74.03 ± 3.79) from the patient group, while it increased in LDL (68.39 ± 2.62 from 52.63 ± 2.09). Typically, the total amount of HDL in CAD patients decreases while LDL increases. Given this trend, oxidation occurred to a great extent in patients. Moreover, the number of oxidized species was newly identified in LDL and VLDL fractions from the patient group, though their relative levels were low. These changes are shown in Figure 4 by plotting the percentage of singly hydroxylated species with respect to the original PL molecule in each lipoprotein class. In addition to the above case (16:0/18:2-PC), the relative

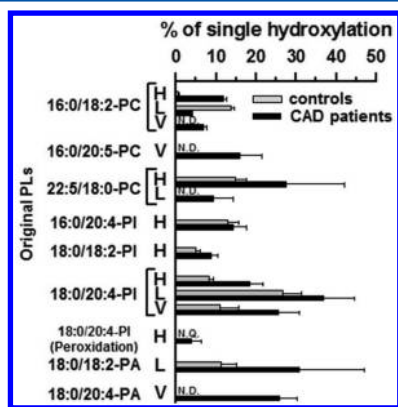


Figure 4. Percentage of singly hydroxylated species compared to the original intact molecule for selected Ox-PL species quantified from control and patient samples. H, L, and V represent HDL, LDL, and VLDL fractions, respectively. N.D., not detected, and N.Q., not quantifiable.

portions of singly hydroxylated species of 22:5/18:0-PC, 18:0/18:2-PI, and 18:0/20:4-PI from HDL, 18:0/18:2-PA from LDL, and 18:0/20:4-PI from VLDL were increased nearly 2-fold. In particular, singly oxidized species of 16:0/20:5-PC and 18:0/20:4-PA were newly identified in the VLDL fraction from the patient group at greater than 16 and 25%, respectively. While hydroperoxylated PL species were detected in this study, most of them were not quantified due to their low concentrations, except 18:0/20:4+OO-PI as shown in Table 3. It can be expected that peroxides added to PLs were relatively unstable, and most of them proceeded to oxidize further to produce hydroxides. From Tables 1 and 3 and Table S1 in the Supporting Information, it can be summarized that the types of acyl chains commonly oxidized are PLs with a saturated acyl chain such as 16:0 or 18:0 in the sn-1 position of the glycerol backbone together with unsaturated acyl chains such as 18:2 or 20:4 in the sn-2 position. Moreover, it was shown that most of the identified Ox-PLs in Table 1 and Table S1 in the Supporting Information underwent oxidation of an unsaturated acyl chain at sn-2; however, Ox-PGs showed oxidations at sn-1 since most PGs identified in this study contained an unsaturated acyl chain in sn-1.

CONCLUSIONS

In this study, Ox-PLs in different lipoprotein classes (HDL, LDL, and VLDL) have been profiled qualitatively and quantitatively by using an off-line combination of semi-preparative scale flow FFF and nLC-ESI-MS/MS. The molecular structures of Ox-PL species were accurately determined from fragment ion spectra by data-dependent CID experiments and selected Ox-PLs of each lipoprotein class were quantitatively analyzed between CAD patients and healthy controls. This study suggests that a proper extraction method is necessary to retrieve the oxidized form of PLs due to the increase in polarity after oxidation along with suitable gradient elution conditions, which can separate relatively polar but low abundance Ox-PLS species from intact PLs, of which the latter can reduce spectral congestion during MS experiments. While the numbers of unique PLs were 283 for the control and 315 for the patient group, those of Ox-PLs without including LPLs were 63 and 105, respectively, showing that oxidation of PLs in CAD patients' lipoproteins were significantly progressed. In particular, more Ox-PL species were newly identified in LDL and VLDL fractions from the patient group, and the relative ratio of singly oxidized PL to the corresponding intact PL molecule was found to be significantly higher for samples from CAD patients compared to those from controls. From structural determinations of Ox-PLs and their quantifications, it was found that singly hydroxylated PLs were more abundant than hydroperoxylated PLs or short chain products, even though a variety of Ox-PLs with truncation of an acyl chain were observed. Moreover, oxidation occurred in most PL molecules having a saturated acyl chain (16:0 or 18:0) mostly at the sn-1 position of the glycerol backbone and an unsaturated acyl chain with at least two double bonds. From the current study, it can be concluded that 16:0/18:2, 16:0/20:4, 18:0/18:2, and 18:0/20:4 were the most common type of acyl chain structures in CAD patient lipoprotein particles.

ASSOCIATED CONTENT

Supporting Information

Additional information as noted in text. This material is available free of charge via the Internet at <http://pubs.acs.org>.

AUTHOR INFORMATION

Corresponding Author

*Phone: 82 2 2123 5634. Fax: 82 2 364 7050. E-mail: mhmoon@yonsei.ac.kr.

Notes

The authors declare no competing financial interest.

ACKNOWLEDGMENTS

This research was supported by Grant NRF-2010-0014046 through the National Research Foundation of Korea (NRF).

REFERENCES

- (1) Parthasarathy, S.; Raghavamenon, A.; Omar, M.; Garelnabi, G.; Santanam, N. *Free Radicals and Antioxidant Protocols*; Springer: New York, 2010.
- (2) Navab, M.; Hama, S. Y.; Ready, S. T.; Ng, C. J.; Van Lenten, B. J.; Laks, H.; Fogelman, A. M. *Lipidology* **2002**, *13*, 363–372.
- (3) Rajman, I.; Kendall, M. J.; Cramb, R.; Holder, R. L.; Salih, M.; Gammage, M. D. *Atherosclerosis* **1996**, *125*, 231–242.
- (4) Austin, M. A.; Rodriguez, B. L.; McKnight, B.; McNeely, M. J.; Edwards, K. L.; Curb, J. D.; Sharp, D. S. *Am. J. Cardiol.* **2000**, *86*, 412–416.
- (5) Adachi, J.; Asano, M.; Yoshioka, N.; Nushida, H.; Ueno, Y. *Kobe J. Med. Sci.* **2006**, *52*, 127–140.
- (6) Ehara, S.; Ueda, M.; Naruko, T.; Haze, K.; Itoh, A.; Otsuka, M.; Komatsu, R.; Matsuo, T.; Itabe, H.; Takano, T.; Tsukamoto, Y.; Yoshiyama, M.; Takeuchi, K.; Yoshikawa, J.; Becker, A. E. *Circulation* **2001**, *103*, 1955–1960.
- (7) Watson, A. D.; Leitinger, N.; Navab, M.; Faull, K. F.; Hörkkö, S.; Witztum, J. L.; Palinski, W.; Schwenke, D.; Salomon, R. G.; Sha, W.; Subbanagounder, G.; Fogelman, A. M.; Berliner, J. A. *J. Biol. Chem.* **1997**, *272*, 13597–13607.
- (8) Borst, J. W.; Visser, N. V.; Kouptsova, O.; Visser, A. J. W. G. *Biochim. Biophys. Acta: Mol. Cell. Biol. Lipids* **2000**, *1487*, 61–73.
- (9) Harrison, K. A.; Davies, S. S.; Marathe, G. K.; McIntyre, T.; Prescott, S.; Reddy, K. M.; Falck, J. R.; Merphy, R. C. *J. Mass Spectrom.* **2000**, *35*, 224–236.
- (10) Vitrac, H.; Courrèlongue, M.; Couturier, M.; Collin, F.; Théron, P.; Rémita, S.; Peretti, P.; Jore, D.; Gardès-Albert, M. *Can. J. Physiol. Pharmacol.* **2004**, *82*, 153–160.
- (11) Reis, A.; Domingues, M. R. M.; Amado, F. M. L.; Ferrer-Correia, A. J.; Domingues, P. *J. Chromatogr., B* **2007**, *855*, 186–199.
- (12) Morgan, L. T.; Thomas, C. P.; Kühn, H.; O'Donnell, V. B. *Biochem. J.* **2010**, *431*, 141–148.
- (13) Clark, S. R.; Guy, C. J.; Scurr, M. J.; Taylor, P. R.; Kift-Morgan, A. P.; Hammond, V. J.; Thomas, C. P.; Coles, B.; Roberts, W.; Eberl, M.; Jones, S. A.; Topley, N.; Kotecha, S.; O'Donnell, V. B. *Blood* **2011**, *117*, 2033–2043.
- (14) Lee, J. Y.; Lim, S.; Park, S.; Moon, M. H. *J. Chromatogr., A* **2013**, *1288*, 54–62.
- (15) Bang, D. Y.; Kang, D.; Moon, M. H. *J. Chromatogr., A* **2006**, *1104*, 222–229.
- (16) Lee, J. Y.; Min, H. K.; Moon, M. H. *Anal. Bioanal. Chem.* **2011**, *400*, 2953–2961.
- (17) Moon, M. H. *Mass Spectrom. Lett.* **2014**, *5*, 1–11.
- (18) Bang, D. Y.; Byeon, S. K.; Moon, M. H. *J. Chromatogr., A* **2014**, *1331*, 19–26.
- (19) Lee, J. Y.; Min, H. K.; Choi, D.; Moon, M. H. *J. Chromatogr., A* **2010**, *1217*, 1660–1666.
- (20) Byeon, S. K.; Lee, J. Y.; Lim, S.; Choi, D.; Moon, M. H. *J. Chromatogr., A* **2012**, *1270*, 246–253.
- (21) Byeon, S. K.; Lee, J. Y.; Moon, M. H. *Analyst* **2012**, *137*, 451–458.
- (22) Lim, S.; Byeon, S. K.; Lee, J. Y.; Moon, M. H. *J. Mass Spectrom.* **2012**, *47*, 1004–1014.